Mediator subunit MDT-15/MED15 and Nuclear Receptor HIZR-1/HNF4 cooperate to regulate toxic metal stress responses in *Caenorhabditis elegans*

Naomi Shomer[1-3,#], Alexandre Zacharie Kadhim[1-3,#], Jennifer Margaret Grants[1-3,#], Xuanjin Cheng[2,3], Amy Fong-Yuk Poon[2,3], Michelle Ying Ya Lee[2,3], Forum Bhanshali[2,3*], Anik Muhuri[2,3], Jung In Park[2,3], Dongyeop Lee[5], Seung-Jae V. Lee[6], Francis Christopher Lynn[3,4,7], and Stefan Taubert[1-4,8]

[1]Graduate Program in Medical Genetics, [2]Centre for Molecular Medicine and Therapeutics, [3]BC Children's Hospital Research Institute, [4]Graduate Program in Cell & Developmental Biology, University of British Columbia, 950 W 28th Ave, Vancouver, BC V5Z 4H4, Canada; [5]Department of Life Sciences, School of Interdisciplinary Bioscience and Bioengineering, ITCE, Pohang University of Science and Technology, 77 Cheongam-Ro, Nam-Gu, Pohang, Gyeongbuk, 37673, South Korea, [6]Department of Biological Sciences, Korea Advanced Institute of Science and Technology, 291 Daehak-Ro, Yuseong-Gu, Daejeon, 34141, South Korea, [7]Department of Surgery, and [8]Department of Medical Genetics, University of British Columbia, 950 W 28th Ave, Vancouver, BC V5Z 4H4, Canada

[*]Current address: Terramera Inc., 333 Seymour St, Vancouver, BC V6B 5A6, Canada

Corresponding author: Stefan Taubert

[#]Authors contributed equally to this work

Keywords: Mediator complex, cadmium, zinc, HNF4α, β-cell

Short title: MDT-15/MED15 and HIZR-1/HNF4 protect against toxic metals

Abstract

Zinc is essential for cellular functions as it is a catalytic and structural component of many proteins. In contrast, cadmium is not required in biological systems and is toxic. Zinc and cadmium levels are closely monitored and regulated as their excess causes cell stress. To maintain homeostasis, organisms induce metal detoxification gene programs through stress responsive transcriptional regulatory complexes. In *Caenorhabditis elegans*, the MDT-15 subunit of the evolutionarily conserved Mediator transcriptional coregulator is required to induce genes upon exposure to excess zinc and cadmium. However, the regulatory partners of MDT-15 in this response, its role in cellular and physiological stress adaptation, and the putative role mammalian for MED15 in the metal stress responses remain unknown. Here, we show that MDT-15 interacts physically and functionally with the Nuclear Hormone Receptor HIZR-1 to promote molecular, cellular, and organismal adaptation to excess metals. Using gain- and loss-of-function mutants and qPCR and reporter analysis, we find that *mdt-15* and *hizr-1* cooperate to induce zinc and cadmium responsive genes. Moreover, the two proteins interact physically in yeast-two-hybrid assays and this interaction is enhanced by the addition of zinc or cadmium, the former a known ligand of HIZR-1. Functionally, *mdt-15* and *hizr-1* mutants show defective storage of excess zinc in the gut, and at the organismal level, *mdt-15* mutants are hypersensitive to zinc- and cadmium-induced reductions in egg-laying. Lastly, mammalian MDT-15 orthologs bind genomic regulatory regions of metallothionein and zinc transporter genes in a metal-stimulated fashion, and human MED15 is required to induce a metallothionein gene in lung adenocarcinoma cells exposed to cadmium. Collectively, our data show that *mdt-15* and *hizr-1* cooperate to regulate metal detoxification and zinc storage and that this mechanism appears to be at least partially conserved in mammals.

Introduction

In their habitats, biological organisms encounter many metals, including essential micronutrients such as iron, zinc, copper, and manganese, and toxic metals such as cadmium, mercury, lead, and arsenic. Zinc is an essential trace element that plays a crucial role in numerous cellular and physiological processes (1). It has a structural role in metabolic enzymes, growth factors, and transcriptional regulators such as zinc finger proteins, and is also an enzymatic cofactor and a signaling molecule (2,3). Accordingly, zinc is necessary for the function of approximately 10% of proteins in the human proteome and approximately 8% of proteins in the nematode worm *Caenorhabditis elegans* (4). In line with its requirement in diverse proteins, zinc deficiency causes a broad range of symptoms and dysfunctions in humans, such as skin and eye lesions, thymic atrophy, diarrhea, defective wound healing, and others (5,6). *Vice versa*, exposure to high doses of zinc is also detrimental, as it has toxic effects, causes cell stress, and alters physiological programs such as systemic growth, immune responses, and neuro-sensory and endocrine functions (5).

Unlike zinc, cadmium is a non-essential toxic metal encountered by biological organisms as a naturally occurring and industrial environmental contaminant. Cadmium has no known function in biological systems, and exposure causes intracellular damage along with the production of reactive oxygen species (7). In humans, cadmium exposure can result in respiratory disease, kidney damage, neurological disorders, and various types of cancers (7,8). Interestingly, zinc and cadmium share a similar electron configuration; thus, cadmium may substitute for zinc at the molecular level, for example as an enzyme cofactor, thus reducing or abrogating normal protein function (9).

Another consequence of the elemental similarity is that the biological responses to and the systemic detoxification of zinc and cadmium are similar (2,5,10,11). Key detoxification and homeostasis components include metal-sequestering proteins such as metallothioneins (MTs), which bind a wide range of metals including cadmium, lead, zinc, mercury, copper, and others. MTs appear to regulate the uptake, transport, and regulation of zinc in biological system, and also scavenge reactive

oxygen species such superoxide (12). Other important detoxification and homeostasis components include transporters such as the cation diffusion facilitators (CDF; also known as zinc transporter (ZnT) or solute carrier 30 (SLC30) family proteins) that transport zinc into the cytoplasm, and the Zrt- and Irt-like proteins (ZIP; aka SLC39A family proteins) that transport zinc out of the cytoplasm (13,14).

To maintain homeostasis in the face of changing metal levels, transcriptional regulatory mechanisms adjust gene expression as needed. Metal-responsive transcription factor-1 (MTF-1) is a transcription factor that is evolutionarily conserved from insects to humans. It binds metal responsive elements (MREs) in the promoters of target genes (e.g. metallothioneins) and activates their expression when metals such as zinc are in excess (15-17). MTF-1 directly senses zinc with its six zinc fingers and with an acidic, metal-responsive transcriptional activation domain; related metals such as cadmium appear not to directly bind MTF-1 and instead are likely detected indirectly through the altered availability of zinc. Additional, unknown transcription factors and/or activation mechanism likely control gene expression in response to excess zinc in these organisms, as some genes are regulated independently of MTF-1 and MREs in such conditions (16,18). Recent studies in *C. elegans*, whose genome lacks a detectable MTF-1 ortholog despite the presence of MREs, revealed that the activation of genes in conditions of high zinc requires the High Zinc Activated (HZA) element and the HZA-binding Nuclear Hormone Receptor high-zinc–activated nuclear receptor 1 (HIZR-1; aka NHR-33) (19,20). HIZR-1 is a sequence homolog of mammalian Hepatocyte Nuclear Factor 4 (HNF4) (20,21), but whether HNF4 proteins regulate gene expression in response to high metal concentrations in mammals remains unknown.

To effectively and specifically activate gene expression, transcription factors require accessory proteins termed coregulators (22-24). One important coregulator is Mediator, a ~30 protein subunit complex that is conserved from yeast to human (25,26). Individual Mediator subunits selectively engage transcription factors and thus regulate specific developmental and physiological gene programs. For example, Mediator subunit MDT-15/Med15 and Mediator kinase cyclin dependent kinase 8 (CDK-

8) are required for many stress and adaptive responses across species (26-31). In the context of heavy metal responsive transcription, *Drosophila melanogaster* MTF-1 requires Mediator for gene activation via MREs in response to excess metals (17,32). In *C. elegans*, we showed that Mediator subunit *mdt-15* is required for the induction of zinc and cadmium responsive genes (33). Others found that zinc-dependent activation via the HZA element required *mdt-15* at one extrachromosomal promoter reporter (19). As MDT-15 is a known coregulator of HNF4-like NHRs in *C. elegans* (34-37), this suggests that MDT-15 may cooperate with the HZA-binding HIZR-1 to adapt gene expression in response to high zinc in *C. elegans*.

Here, we tested whether MDT-15 and HIZR-1 cooperate to regulate zinc and cadmium responsive transcription in *C. elegans* and whether MED15, the mammalian ortholog of MDT-15, also participates in heavy metal stress responses. Because the Mediator kinase CDK-8 regulates transcriptional stress responses (30,31), we also assessed the function of *C. elegans cdk-8* in metal responsive transcription. Using genetic, molecular, cytological, and functional assays, we find that MDT-15 and HIZR-1 interact physically and functionally in zinc and cadmium stress responses, and that mammalian MED15 is recruited to metal responsive genes and required for metal-induced gene expression.

Results

mdt-15 and *cdk-8* are necessary for cadmium- and zinc-induced gene activation

We previously showed that *mdt-15* is required to induce the mRNA levels of several genes in response to high levels of zinc and cadmium (33). In line with this finding, genes downregulated in *mdt-15(tm2182)* hypomorph mutants showed significant overlap with cadmium-induced genes (Fig 1A). Similarly, cadmium-induced genes overlap significantly with genes downregulated in *cdk-8 (tm1238)* null mutants (Fig 1B), suggesting that *cdk-8* plays a similar role as *mdt-15*. To test the requirement of *cdk-8* in cadmium detoxification and to assess its role in the zinc response, we used real-time quantitative PCR (qPCR) to measure the mRNA levels of metallothioneins (*mtl-1, mtl-2*), zinc transporters (ZnT) implicated in cadmium and zinc detoxification (*ttm-1, cdf-2*), and the cadmium responsive gene *cdr-1* (10,20,33). Comparing wild-type worms and *cdk-8(tm1238)* mutants, we observed a significant decrease of *cdr-1* mRNA levels upon exposure to cadmium and of *mtl-2* mRNA levels upon exposure to zinc; other metal responsive genes showed a similar trend but were not significantly altered (Fig 1C-D). Thus, *cdk-8* is required for maximal gene expression in response to zinc or cadmium, but this requirement is less prevalent and substantial than the one we previously observed for *mdt-15* (33).

hizr-1 and *elt-2* are required to induce the *cdr-1* promoter

To delineate the mechanism of MDT-15 and CDK-8 driven, cadmium and zinc responsive transcription, we generated a transcriptional *cdr-1p::gfp* reporter, encompassing 2.8 kb of the *cdr-1* promoter (Fig 2A). We chose *cdr-1* as a model because it is highly cadmium and zinc responsive and requires *mdt-15* and *cdk-8* for activation (10,33,38), suggesting that it might be a good tool to identify DNA regulatory elements and cognate transcription factors that cooperate with these Mediator subunits. As expected (10,33,38), we observed weak basal expression of this reporter, but substantial induction of fluorescence by 200μM zinc and 100μM cadmium (Fig S1A-B); expression was primarily

localized to the intestine (Fig S1A-B), as expected (10,38). Knockdown of *mdt-15* by feeding RNA interference (RNAi) caused a significant decrease in basal *cdr-1p::gfp* fluorescence and abrogated fluorescence induction by cadmium and zinc (Fig 2B). Similarly, *cdk-8(tm1238); cdr-1p::gfp* worms showed a significant decrease in basal and metal-induced fluorescence (Fig 2B).

To identify transcription factors that cooperate with *cdk-8* and *mdt-15* to regulate cadmium and zinc responsive transcription, we searched for DNA regulatory elements in the *cdr-1* promoter. We identified candidate elements recognized by SKN-1/Nrf2 (antioxidant response element, ARE), HSF-1 (heat shock response element, HSE), DAF-16/FOXO (DAF-16 binding element, DBE), ELT-2 (GATA element), and HIZR-1 (HZA element), as well as four MREs, which no *C. elegans* transcription factor is yet known to bind (Fig 2A). RNAi analysis revealed that *skn-1*, *hsf-1*, and *daf-16* are not required for *cdr-1* induction by cadmium; *daf-16* depletion actually hyper-induced the *cdr-1p::gfp* promoter (Fig 2C). In contrast, knocking down *elt-2* or *hizr-1* abrogated fluorescence induction (Fig 2C). As *elt-2* is required for intestinal development (39), we examined post-developmental *elt-2* knockdown, which also caused abrogation of basal and cadmium-induced *cdr-1p::gfp* expression (Fig S1C). Thus, *elt-2* is required at the *cdr-1* promoter independently of its role in development.

We confirmed the requirements for *elt-2* and *hizr-1* by site-directed mutagenesis of their cognate DNA elements. We generated substitution mutations in the HZA (*mutHZA*) or GATA sites (*mutGATA1* and *mutGATA2*) of the *cdr-1p::gfp* reporter (Fig 2A). Each mutation individually caused a significant decrease in cadmium-induced promoter activity compared to the wild-type *cdr-1p::gfp* reporter; mutations in the HZA elements also caused a significant decrease in the basal activity of the *cdr-1p::gfp* reporter (Fig 2D). Collectively, these data show that Mediator subunits MDT-15 and CDK-8 and the transcription factors ELT-2 and HIZR-1 are required to control expression from the cadmium/zinc-inducible *cdr-1* promoter.

***mdt-15* and *hizr-1* function is co-dependent**

Based on the above data, we hypothesized that MDT-15 and/or CDK-8 might interact functionally and physically with HIZR-1 and/or ELT-2 to activate metal-induced transcription. To examine a putative functional relationship between MDT-15 and HIZR-1, we studied the *hizr-1(am285)* D270N gain-of-function (gf) mutant that induces zinc responsive genes even in the absence of zinc (20). In line with published data (20), qPCR analysis revealed induction of *cdr-1*, *mtl-1*, *mtl-2*, and *cdf-2* in *hizr-1(am285)* mutants grown on control RNAi; importantly, *mdt-15* RNAi significantly reduced or abrogated these inductions (Fig 3A). Next, we studied the *mdt-15(et14)* P117L gain-of-function (gf) mutation that induces MDT-15 regulated lipid metabolism genes (40). Because this mutation is closely linked to a *paqr-1(3410)* loss-of-function mutation, which it suppresses (40), we used the *mdt-15(yh8)* strain, which was generated by CRISPR and carries P117L alone (41). The *mdt-15(yh8)* gf mutation was sufficient to induce *mtl-1* and *mtl-2* (Fig 3B); RNAi experiments revealed that *mtl-2* induction required *hizr-1*, with a similar trend for *mtl-1* (Fig 3B). In contrast, *nhr-49*, which cooperates with MDT-15 to activate lipid metabolism and stress response genes (34,36), was not required to induce metal-responsive genes in the *mdt-15(yh8)* mutant (Fig 3B). We conclude that MDT-15 and HIZR-1 interact specifically to induce metal responsive genes *in vivo*.

MDT-15 physically interacts with HIZR-1 in zinc-enhanced fashion

The above data suggest that MDT-15 might interact physically with HIZR-1, as shown for other *C. elegans* HNF4-like NHRs (34,35). To test whether HIZR-1 binds MDT-15, we used the yeast-two-hybrid (Y2H) system. First, we examined the interaction between a full length HIZR-1 prey and a MDT-15-ΔCT bait (aa 1-600); full-length MDT-15 (aa 1-780) autoactivates and cannot be used as bait in Y2H assays (see (42) for details). In these assays, MDT-15 and HIZR-1 showed a statistically significant interaction that was similar in strength to the interaction of the MDT-15-ΔCT bait with a SKN-1c prey (positive control (42); Fig 3C).

The HIZR-1 ligand binding domain (LBD) binds zinc in the micromolar range, suggesting that zinc is a *bona fide* ligand for HIZR-1 (20). We hypothesized that the addition of zinc might enhance the interaction of HIZR-1 with MDT-15, as shown for other many other ligand-stimulated NHR-coregulator interactions. Indeed, addition of zinc enhanced the interaction between MDT-15 and HIZR-1, with significant effects at low micromolar concentrations (Figs 3D, S2A). As *mdt-15* also contributes to cadmium-induced gene expression, we tested whether this metal also enhanced MDT-15 binding to HIZR-1 and found that this was the case (Fig 3D). In contrast, manganese did not enhance the binding of MDT-15 with HIZR-1 (Fig 3D).

NHRs contain a zinc-finger DNA binding domain (DBD), suggesting that zinc-stimulated binding to a coregulator such as MDT-15 might be a common feature of NHRs. To examine the specificity of zinc- and cadmium-stimulated MDT-15–NHR interaction, we examined whether these metals alter the binding of two other known MDT-15 binding partners, NHR-64 and NHR-49 (34). We found that NHR-64 interacts with MDT-15 as strongly as HIZR-1 does in the presence of zinc or cadmium, while NHR-49 binding to MDT-15 mimics the interaction of HIZR-1 and MDT-15 in the absence of zinc; importantly, neither NHR-64 nor NHR-49 binding to MDT-15 was altered by supplementation with zinc, cadmium, or manganese at eth concentrations that significantly enhanced binding of HIZR-1 to MDT-15 (Fig 3D). We conclude that metal-stimulation of MDT-15 interaction is not a general feature of NHRs but specific to HIZR-1.

Binding determinants in MDT-15 and HIZR-1

MDT-15 contains an N-terminal KIX-domain that binds several NHRs and the lipogenic transcription factor SBP-1 (34,35,43). Thus, we hypothesized that MDT-15 might physically bind HIZR-1 through the KIX-domain (aa 1-124; Fig S2B). To test this hypothesis, we assayed binding of HIZR-1 to an MDT-15-KIX-domain and to an MDT-15ΔCT variant lacking the KIX-domain (MDT-15ΔKIXΔCT; aa 125-600). The binding of HIZR-1 to the MDT-15-KIX-domain was similar to the

binding to MDT-15ΔCT; in contrast, MDT-15ΔKIXΔCT was unable to bind HIZR-1 (Fig S2C). This indicates that the KIX-domain is necessary and sufficient for the HIZR-1–MDT-15 interaction.

The *hizr-1(am285)* gf mutation is an aspartate 270 to asparagine (D270N) substitution that results in increased nuclear localization and constitutive activation of zinc responsive genes even in the absence of zinc (20). Sequence comparison revealed that D270 is conserved in the HIZR-1 orthologs of three other species in the *Caenorhabditis* genus (Fig S2D), suggesting that it may be functionally important. We hypothesized that the D270N mutation might affect MDT-15 binding. To test this, we performed Y2H assays with a HIZR-1-D270N prey generated by site-directed mutagenesis. HIZR-1-D270N interacted more strongly with MDT-15 than did HIZR-1-WT, resembling in strength the WT HIZR-1–MDT-15 interaction in the presence of zinc (Fig 3E). Nevertheless, supplemental zinc further enhanced this interaction (Fig 3E), suggesting that, D270 does not mimic the effects of zinc-stimulated binding.

mdt-15(tm2182) mutants display zinc storage defects and are hypersensitive to zinc and cadmium

To test whether the defects of *mdt-15(tm2182)* mutants in metal responsive transcription have functional consequences, we studied two phenotypes: cellular zinc storage and egg-laying. At the cellular level, gut granules store zinc when it is present in excess, thus protecting cells; *vice versa*, they replenish zinc in situations of zinc deficiency (44). To study zinc storage in gut granules in wild-type and mutant worms, we used the zinc-specific fluorescent dye FluoZin-3 (44). We observed little difference between wild-type, *mdt-15(tm2182)*, *cdk-8(tm1238)*, and *hizr-1(am286)* mutants in "normal" conditions, i.e. without zinc supplementation (Fig S3A-C). Wild-type worms supplemented with 200mM zinc showed bigger granules with a stronger FluoZin-3 signal (Fig 4A), as reported (44). Strikingly, *mdt-15(tm2182)* mutants displayed significantly fewer gut granules in high zinc conditions than wild-type worms and *cdk-8(tm1238)* mutants (Fig 4A-B). As HIZR-1 interacts with MDT-15 in

239 zinc-stimulated fashion, we also studied *hizr-1(am286)* null mutants and found that they also have less
240 granules than wild-type worms in conditions of excess zinc (Fig 4C).

241 *mdt-15(tm2182)* mutants show reduced expression of several fatty acid metabolism enzymes,
242 especially fatty acid desaturases such as *fat-6/stearoyl-CoA desaturase*. This causes defects in cell
243 membrane fatty acid desaturation and directly underlies numerous phenotypes caused by *mdt-15*
244 deficiency, including slow growth, reduced body size, and short life span (34,41,43,45,46). Altered
245 membrane lipids in *mdt-15(tm2182)* mutants could cause organelle dysfunction and conceivably affect
246 zinc storage. Thus, we tested whether *fat-6/stearoyl-CoA desaturase* depletion by RNAi causes defects
247 in zinc storage (note that *fat-6* depletion also deletes the highly homologous gene *fat-7* (47)). In
248 contrast to *mdt-15(tm2182)* mutants, however, *fat-6(RNAi)* worms did not show any overt defects in
249 zinc storage in high zinc conditions (Fig S3D-E). This suggests that the zinc storage defects observed
250 in the *mdt-15(tm2182)* mutants are not due to altered membrane composition and function.

251 We also assessed the effect of excess zinc and cadmium on an organismal phenotype, egg-
252 laying (Fig 4D). We found that 100µM zinc decreased the number of eggs laid by wild-type worms by
253 approximately 30 percent; in contrast, the same concentration of zinc almost completely abolished egg-
254 laying in *mdt-15(tm2182)* mutants, indicating that this mutant is hyper-sensitive to zinc. Similarly,
255 2.5µM cadmium reduced the number of eggs laid by wild-type worms by approximately 20 percent,
256 but almost completely abrogated it in *mdt-15(tm2182)* mutants (Fig 4E), indicating that this mutant is
257 hyper-sensitive to cadmium. Thus, *mdt-15(tm2182)* mutants are less able than wild-type to resist excess
258 heavy metals at an organismal level.

259

260 **Mammalian MED15 may also regulate metal-induced transcription**

261 To test whether *mdt-15*'s role in regulating metal-responsive transcription is conserved in
262 mammals we studied the role its human and mouse orthologs, MED15 and Med15 (48), in two cell
263 lines. First, we studied A549 human epithelial lung adenocarcinoma cells, because cadmium increases

lung cancer risk and induces a heavy metal stress response in this cell line (49-51). We depleted MED15 in A549 cells by transfecting small interfering RNAs (siRNAs) targeting MED15 (*vs.* scrambled control), and then exposed the transfected cells to 5μM cadmium for 4 hours. Using qPCR, we found that cadmium induced the metallothioneins MT1X and MT2A, orthologues of *C. elegans mtl-1* and *-2*, respectively (Fig 5A). Notably, while MT1X was unaffected, MT2A induction was completely blocked by MED15 depletion (Fig 5A), suggesting that MED15 is required to induce at least this one gene in response to heavy metal exposure. To test whether MED15 binds to the promoter of MT2A, we performed chromatin immunoprecipitation followed by qPCR (ChIP-qPCR), assessing MED15 occupancy before and after the addition of 5μM cadmium to the extracellular media. We found that MED15 was recruited preferentially to the promoter of MT2A after addition of 5μM cadmium (Fig 5B).

We also studied the MIN6 mouse insulinoma cell line because the insulin-secreting β-cells of the mammalian pancreas require zinc for insulin crystallization and contain among the highest levels of zinc in the body (14,52,53). ZnT8/SLC30A8, the mouse ortholog of the MDT-15 and HIZR-1 regulated zinc transporter CDF-2 (44), is expressed highly in the in α- and β-cells of the endocrine pancreas (14). To test whether the expression of mouse *Slc30a8* and metallothionein genes are induced by excess zinc, we exposed MIN6 cells to 50μM zinc for 24 hours and assessed expression by qPCR. We observed that *Slc30a8*, *Mt1*, and *Mt2* are zinc responsive, whereas *Med15* expression did not increase (Fig 5C). To test whether Med15 directly binds to the promoters of *Slc30a8* and *Mt1*, we performed chromatin immunoprecipitation followed by qPCR (ChIP-qPCR), assessing Med15 occupancy before and after the addition of excess zinc to the extracellular media. We found that Med15 was recruited to the promoters of both *Slc30a8* and *Mt1* in excess zinc (Fig 5D). Collectively, these experiments suggest that mammalian MED15 proteins directly bind the promoters of metal stress responsive genes and are required for the induction of at least one cadmium responsive gene in lung adenocarcinoma cells.

289 **Discussion**

290 Organisms encounter both essential and toxic metals in their habitant and must allow adequate
291 uptake of necessary micronutrients while secreting/sequestering excess amounts of micronutrients and
292 toxic metals. *C. elegans* lacks the MTF-1 protein that regulates metal responsive transcription in many
293 animals. Instead, it utilizes the Nuclear Hormone Receptor HIZR-1 to control the response to excess
294 zinc (20). Here, we show that the *C. elegans* Mediator subunit MDT-15 interacts physically and
295 functionally with HIZR-1, that loss of *mdt-15* alters storage of excess zinc *in vivo*, and that *mdt-15*
296 mutants are hypersensitive to zinc and cadmium. Moreover, mammalian MED15 is recruited to
297 regulatory elements of metal-responsive genes in metal-stimulated fashion, and MED15 depletion
298 blocks the induction of a cadmium responsive gene in lung adenocarcinoma cells. Thus, the HZA
299 element, HIZR-1 transcription factor, and MDT-15 coregulator compose a regulatory mechanism that
300 adapts gene expression in response to excess zinc and cadmium to protect the host organism (Fig 6).
301 This regulatory mechanism represents a new partnership between a *C. elegans* NHR and the
302 coregulator MDT-15 that regulates one particular adaptive response, that to excess heavy metals.
303 Moreover, this metal stress response mechanism appears to be at least partly conserved in mammalian
304 cells (Fig 6).

305

306 **MDT-15 is a coregulator of HIZR-1**

307 Because *C. elegans* appears to lack an MTF-1 ortholog, it has been unclear how it regulates
308 gene expression in response to changing levels of various metals. We previously showed that the
309 Mediator subunit *mdt-15* is essential for both zinc and cadmium activated transcription (33), and the
310 Kornfeld laboratory identified the HZA element and its cognate TF HIZR-1 as regulators of zinc-
311 inducible transcription (19,20). This raised the hypothesis that these three components might all
312 cooperate mechanistically; alternatively, they might act in separate molecular pathways. Here, we
313 provide multiple lines of evidence that HIZR-1 and MDT-15 cooperate mechanistically to induce gene

314 expression in excess zinc and cadmium. First, *mdt-15*, *hizr-1*, and the HZA element are required to
315 activate the *cdr-1p::gfp* reporter, i.e. they phenocopy (Fig 2; see also (19,20)). Second, MDT-15 and
316 HIZR-1 physically interact in the yeast-two-hybrid system; notably, this binding can be stimulated by a
317 known ligand of HIZR-1 (zinc; (20)) and requires a known NHR binding domain of MDT-15 (the KIX-
318 domain; (34,35); Fig 3). Third, genetic gain of *hizr-1* or *mdt-15* function confers metal homeostasis
319 gene activation that requires the reciprocal partner (Fig 3). Fourth, loss of *mdt-15* and *hizr-1* causes
320 similar defects in zinc storage and renders worms hypersensitive to zinc (Fig 4 and (20)). Although we
321 cannot exclude that the GATA factor ELT-2, which also activates zinc responsive genes including *cdr-*
322 *1* (Fig 2 and (19)), may interact with MDT-15, we have not observed an interaction between ELT-2 and
323 MDT-15 in our yeast-two-hybrid assays. Based on our new and published data, we propose a model
324 whereby elevated levels of zinc or cadmium promote the formation of a HIZR-1–MDT-15 regulatory
325 complex, which acts through the HZA element to induce the expression of genes required for metal
326 homeostasis (Fig 6).
327
328 **MDT-15 binds HIZR-1 in metal-stimulated fashion**
329 Interestingly, zinc or cadmium supplementation enhanced MDT-15–HIZR-1 binding (Fig 3).
330 This suggests that, besides promoting HIZR-1 nuclear translocation (20), these metals also modulate
331 the TF-Mediator interaction, a classical feature of *bona fide* NHR ligands (54). Importantly, two other
332 HNF4-related NHRs that also bind MDT-15 (34) did not show metal-enhanced binding. This agrees
333 with the notion that zinc is a specific ligand of HIZR-1 (20) and is not involved in the MDT-15–NHR
334 interactions through the zinc-containing DBDs of NHRs (21).
335 In the Y2H system, we observed increased binding between HIZR-1 and MDT-15 in the low
336 micromolar range of zinc and cadmium. Murine ZIP4 undergoes zinc-stimulated endocytosis when
337 zinc is present in the low micromolar range (55). Similarly, various human and mouse ZIP proteins
338 promote zinc transport in the low micromolar range (56). Thus, the concentration of zinc required to

339 modulate the HIZR-1–MDT-15 interaction resembles that known to engage other zinc homeostasis
340 proteins. This argues that the zinc-modulation of the protein interaction we observed in the Y2H system
341 is likely relevant physiologically.

342 Other physical interactions are likely involved in this zinc homeostasis mechanism, potentially
343 linking HIZR-1 or MDT-15 to ELT-2 or CDK-8, which we found modestly affects metal regulated
344 genes (Fig 1). In addition, HNF4-like NHRs form both homo and heterodimers (21). It would be
345 interesting to examine whether HIZR-1 forms homo- or heterodimers and whether such interactions are
346 modulated by zinc.

347

348 ***mdt-15* protects worms from excess zinc and cadmium**

349 In the *C. elegans* intestine, zinc is stored in lysosome-related organelles called gut granules. In
350 excess zinc conditions, gut granules import surplus zinc via the CDF-2 transporter (44), while zinc is
351 likely also sequestered by MTL-1 and -2. MDT-15 and HIZR-1 promote the induction of these genes
352 when zinc is in excess. This induction is likely physiologically relevant as mutation of either factor
353 results in reduced zinc storage in gut granules and reduced organismal metal tolerance (Fig 4 and (20)).

354 The study that established zinc as a direct ligand for HIZR-1 did not test whether this NHR also
355 bound cadmium (20). Our data suggest that this may be the case, as cadmium stimulates MDT-15–
356 HIZR-1 binding as strongly as does zinc (Fig 3), and *mdt-15* mutants were sensitive to both metals (Fig
357 4). However, we note that cadmium could also act indirectly be displacing zinc from other molecular
358 sites and thus making it available for HIZR-1, resulting in higher available zinc levels that indirectly
359 engage the MDT-15–HIZR-1 complex. It will be interesting to define whether HIZR-1 is indeed a
360 direct sensor of the pollutant cadmium.

361 MDT-15 also promotes oxidative stress responses (36,37,42) and it is conceivable that this
362 function helps protect worms in conditions of excess metals, as e.g. cadmium exposure provokes the
363 formation of reactive oxygen species (7,49). It will be interesting to determine whether HIZR-1

regulates genes other than those involved in storing and mobilizing zinc, such as general or oxidative stress protective genes.

Mammalian MED15 also regulates heavy metal stress responsive gene transcription

C. elegans MDT-15 plays an important role in many adaptive and stress response pathways. Of those, its role in regulating lipid metabolism appears to be conserved in yeast and in mammals (43,57), and its requirement in detoxifying xenobiotic molecules is conserved in fungi (28,58). However, whether mammalian MED15 proteins regulate stress responses was not known. Studying a lung adenocarcinoma cell line that responds to cadmium, we found that MED15 depletion compromises the induction of a metallothionein and that MED15 directly binds the genomic regulatory region of this gene in cadmium enhanced fashion. Similarly, mouse Med15 showed zinc induced binding to the regulatory regions of two genes in MIN6 insulinoma cells; although we did not succeed in effectively depleting Med15 in these cells with transfected siRNAs (not shown), we found that these genes are induced by zinc. Thus, we speculate that the increased binding of Med15 likely upregulates their expression in high zinc. In turn, this likely promotes the protection of MIN6 cells from high zinc (Fig 6). A similar mechanism may protect pancreatic islet β-cells from the transiently high zinc levels these cell experience during insulin exocytosis (52,53).

Currently, we do not know what transcription factor cooperates with mammalian MED15 proteins in metal responsive gene expression. MTF-1 induces cadmium responsive genes in mammals and interacts with Mediator (17), although it is not known which, if any, Mediator subunit directly targets MTF-1. *C. elegans* HIZR-1 is by sequence most closely related to mammalian HNF4α, but functionally and structurally may also resemble mammalian PPARα (21,59). In mouse livers, exposure to the PPARα agonist Wy-14,643 induces *Mt1* and *Mt2* mRNA levels; however, induction is modest (approximately 1.8 fold) and delayed (after 72 hours) (60). Thus, this may well represent an indirect

regulatory effect. Additional work is required to determine the mechanisms by which Mediator, and potentially MED15, regulate gene expression in response to high concentrations of metals in mammalian cells and tissues.

In sum, our work highlights the HZA–HIZR-1–MDT-15 regulatory mechanism as a critical transcriptional adaptive mechanism to excess zinc and cadmium in *C. elegans*, with a potentially conserved role for mammalian MED15.

Materials and Methods

C. elegans transcriptome analysis by microarrays

Microarray transcriptome analysis of the *cdk-8(tm1238)* mutant has been described previously (61). The transcriptome analysis of the *mdt-15(tm2182)* mutant was identical to the analysis of the *cdk-8(tm1238)* mutant using Agilent one-color arrays. We identified a total of 1896 spots with an adjusted P-value of 0.05 or less and a fold-change of >2, representing 798 downregulated and 422 upregulated genes. Microarray data have been deposited in Gene Expression Omnibus. Transcriptome profiles of wild-type worms exposed to 100µM cadmium have been described (62). We determined the overlaps between these datasets and calculated the significance of the overlap as described (36).

C. elegans strains and growth conditions

C. elegans strains were cultured using standard techniques as described (63) at 20°C; all strains used here are listed in Table S1. Nematode growth medium (NGM)-lite (0.2% NaCl, 0.4% tryptone, 0.3% KH_2PO_4, 0.05% K_2HPO_4) agar plates, supplemented with 5µg/mL cholesterol, were used unless otherwise indicated. *Escherichia coli* OP50 was the food source, except for RNAi, for which we used HT115. Zinc ($ZnSO_4$) and cadmium ($CdCl_2$) were supplemented in noble agar minimal media (NAMM; (44)) and NGM-lite plates, respectively, at indicated concentrations. For qPCR and phenotype analysis, we synchronized worms by standard sodium hypochlorite treatment and starvation of isolated eggs on unseeded NGM-lite plates; the next day, synchronized L1 larvae were collected, placed on seeded plates at the desired densities, and grown until being harvested at the desired developmental stage, as indicated.

Gene knockdown by feeding RNAi in *C. elegans*

Knockdown by feeding RNAi was carried out on NGM-lite plates with 25µg/mL carbenicillin, 1mM IPTG, and 12.5µg/mL tetracycline, and seeded twice with the appropriate HT115 RNAi bacteria

clone from the Ahringer library (Source BioScience 3318_Cel_RNAi_complete). RNAi clones were Sanger sequenced to confirm insert identity. RNAi negative control was empty vector L4440. RNAi clones are listed in Table S2.

RNA isolation and quantitative real-time PCR analysis

For *C. elegans*, RNA was extracted from developmentally synchronized worms and prepared for gene expression analysis by real-time PCR analysis as described (61). In all samples, we normalized the expression of the tested genes to the average of three normalization genes: *act-1*, *tba-1*, and *ubc-2*. For A549 cells, RNA was extracted with RNeasy Mini Kit (Qiagen #74106) according to the manufacturer's protocol and converted into cDNA for gene expression analysis by real-time PCR analysis as described (Grants et al. 2016). The expression of the tested genes was normalized to the average of three normalization genes: 18S rRNA, GAPDH, and GUSB. We used t-tests (two-tailed, equal variance) or nonparametric tests to calculate the significance of expression changes between conditions, as indicated. Statistical tests were performed based on recommendations by GraphPad Prism 7. qPCR primers were designed with Primer3web (64) and tested on serial cDNA dilutions, as described (61). Primer sequences are listed in Table S3.

Analysis of the *C. elegans cdr-1* promoter and construction of the *cdr-1p::gfp* promoter reporter

Sequences of regulatory elements involved in the zinc, cadmium, or other detoxification/stress responses were identified from the literature, including ARE, MRE, HSE, DBE, HZA, GATA, and TATA box elements (19,65-74). If available, the equivalent *C. elegans* consensus sequence for each regulatory element was identified in the literature, otherwise the eukaryotic consensus sequence was used. The *cdr-1* promoter (-2853 nucleotides upstream from the predicted transcriptional starting site) was then searched for presence of these candidate elements using SerialCloner 2.5.

The *cdr-1p::gfp* reporter was generated by PCR amplification of the genomic region from 2853 base pairs upstream to 11 base pairs downstream of the *cdr-1* start codon (a G>C mutation at the +3 nucleotide was introduced in the reverse primer to mutate the *cdr-1* start codon) using the primers gtcgacTTTGACGATGACAGAAGAAATG and ggatccTGAATCCAAGATACTTGAGACAGT, followed by BamH1-SalI cloning into pPD95.77 GFP (Addgene #1495) to generate SPD771 (cdr-1p-pPD95.77). Mutant transgenes were generated by site-directed mutagenesis of SPD771 using the Q5 Site-Directed Mutagenesis kit (NEB E0554S) and primers cdr-1p_delGATA1F (CCCTACTTTCccgctgCATTATGTCATCGGG) and cdr-1p_delGATA1R (GTTTCTGTTTCAATTGCAGAATAC) to generate SPD803 (cdr-1p-pPD95.77_DEL_GATA1); cdr-1p_delGATA2F (CCCTACTTTCccgctgCATTATGTCATCGGG) and cdr-1p_delGATA2R (AGAACTGTGTTTTGTGATAAAATTATTG) to generate SPD804 (cdr-1p-pPD95.77_DEL_GATA2); fwd _cdr-1p_delHZA (tcgtggcAATTTTATCACAAAACACAGTTC) and fwd _cdr-1p_delHZA (ccctcaccTCAATTGCAGAATACCATTTG) to generate SPD884 (pPD95.77-cdr-1PmutHZA); and fwd_cdr-1p_delDAF16 (ccgtCCAGAAAGCTTAAAATTCAAG) and /rev_cdr-1p_delDAF16 (gtggAACGGAAAAATATAATATGTATATACAC) to generate SPD879 (pPD95.77-cdr-1PΔDBE). All plasmids were verified by Sanger sequencing. Transgenic strains were generated by injecting a mixture of 50ng/µl GFP reporter plasmid, 5 ng/µl pCFJ90*[myo-2p::mCherry]*, and 95 ng/µl pPD95.77 empty vector into wild-type worms, and then selecting transgenic mCherry-positive progeny.

Staining of *C. elegans* gut granules with FluoZin-3

FluoZin-3 acetoxymethyl ester (Molecular Probes F24195) was reconstituted in dimethylsulfoxide (DMSO) to a 1mM stock solution. FluoZin-3 was diluted in M9 to generate a concentration of 30µM and dispensed on NAMM plates, as described (44). Synchronized wild-type and mutant L4 stage worms were transferred from NGM-lite plates to these plates and cultured for 16 hrs.

469 Worms were then transferred to NGM-lite plates without FluoZin-3 for 30 min to reduce excess
470 FluoZin-3 signal from the intestinal lumen before imaging.
471
472 **Fluorescence microscopy on *C. elegans***
473 For imaging, worms were transferred onto 2% (w/v) agarose pads containing 15µM sodium
474 azide (NaN_3). For the analysis of worms bearing the *cdr-1p::gfp* reporter, the worms were imaged
475 using differential interference contrast (DIC) and fluorescence optics through an HQ camera
476 (Photometrics, Tucson, AZ, USA) on a Zeiss Axioplan 2 microscope (Carl Zeiss Microscopy,
477 Thornwood, NY, USA). Analysis of fluorescence intensity was performed using ImageJ software,
478 normalizing for area and background fluorescence.
479 For analysis of FluoZin-3 stained worms, we used a Leica SP8 confocal microscope with Leica
480 LAS X software. Images of worms with different genotypes were taken with the same exposure times.
481 To assess zinc storage, we quantified the number of FluoZin-3 stained granules in the first six cells of
482 the gut with ImageJ2 (75). To eliminate non-specific fluorescence, we manually removed background
483 signal outside of the gut cells and in the gut lumen. Background fluorescence in the remaining part of
484 the image was then subtracted equally from all images, and images were smoothed with the "Sigma
485 Filter Plus" (edge-preserving noise reduction) function. Images were simultaneously adjusted with
486 Auto threshold of "MaxEntropy" and Auto local threshold of the mean. After adjusting the threshold
487 and reducing background noise, granules where counted automatically with the "3D Objects Counter"
488 function. To verify the automatic count, we manually counted the number of granules in randomly
489 sampled images.
490
491 ***C. elegans* egg laying assay**

N2 and *mdt-15(tm2182)* worms were grown from late L4 stage for 24 hours on agar A plates seeded with OP50 and supplemented with 100μM zinc. Eggs and L1 progeny were counted after that time and compared to worms grown on agar A plats with no additional treatment.

Yeast-two-hybrid assays and Western blots

MDT-15 bait plasmids and NHR-49 and SKN-1c prey plasmids have been described (42). The wild-type HIZR-1 cDNA sequence was amplified with the primers fwd_BamHI_NHR-33_preyY2H (ggatccATGCAAAAAGTTATGAATGATCCTG) and rev_XhoI_NHR-33_preyY2H (ctcgagATCATTTTTCGTATGAACAATGCAC), and cloned into the BamH1 and SalI sites of pGADnewMCS to generate SPD885 (pGADnewMCS_NHR-33). We then used the NEB Q5 site-directed mutagenesis kit (E0554S), template SPD885, and primers SDM_nhr-33-am285_F (AGCAGAAaATGCTGCAAAAAT) and SDM_nhr-33-am285_R (GATTGTACACCCTCTGCATTC) to generate SPD918 (pGADnewMCS_NHR-33_am285). All plasmids were sequenced to verify the accuracy of the sequence amplified by PCR and the absence of other mutations. Pairs of plasmids were transformed into strain Y187 (Clontech, Mountain View, CA, USA) and liquid β-galactosidase assays were performed using an OMEGASTAR plate reader (BMG Labtech, Ortenberg, Germany), as described (42). Each assay included at least three technical replicates and was repeated three or more times. Yeast lysis, SDS-PAGE, and Western blots to detect protein expression were done as described (42). Antibodies used were GAL4 AD Mouse Monoclonal Antibody (Takara Bio USA, Inc. #630402), GAL4 DNA-BD Mouse Monoclonal Antibody (Takara Bio USA, Inc. #630403), and GAPDH Mouse Monoclonal Antibody (CB1001-500UG 6C5) for normalization.

Mammalian cell culture and transfection

A549 lung adenocarcinoma cells were obtained from ATCC and maintained in Dulbecco's Modified Eagle Medium (DMEM; Gibco #11995065) supplemented with 10% fetal bovine serum

(FBS; Gibco #12484028), as described (51). The cells were seeded at a density of $5x10^4$ cells per well in 24-well plates 24 hours before transfection. On the day of transfection, scrambled (Dharmacon #D-001206-13-05) and MED15 specific (Dharmacon #M-017015-02-0005) siRNAs were delivered into A549 cells using DharmaFECT 1 Transfection Reagent (Dharmacon #T-2001-03) according to the manufacturer's protocol. The transfection medium was replaced with complete medium after 24 hours, and the cells were treated with 5μM $CdCl_2$ for hours 48 hours post-transfection. MIN6 cells were cultured in 25mM glucose DMEM, as described (76), and zinc stimulation was performed by addition of 50μM $ZnSO_4$ for 24 hours.

ChIP in A549 and MIN6 cells

ChIP was performed as described (77) in A549 and MIN6 cells with minor modifications. Briefly, cells were grown for 24 hours with or without 50μM $CdCl_2$ and 100μM $ZnSO_4$ (respectively) to $2x10^7$ cells per plate, and crosslinked by adding paraformaldehyde to a final concentration of 3% for 10 minutes at room temperature. Immunoprecipitation was performed using MED15 antibody (ProteinTech, 11566-1-AP). Crosslinking was then reversed by overnight incubation at 65°C and DNA purified using QIAquick PCR purification column (Qiagen, 28104). Immunoprecipitated DNA was then quantified via Qubit (ThermoFisher, Q32854) and analyzed by qPCR for appropriate genomic regulatory loci and controls. Primer sequences are listed in Table S3.

Acknowledgements

We thank the Taubert lab and Dr. Frédéric Picard (Université Laval) for comments on the manuscript. Some strains were provided by the CGC, which is funded by NIH Office of Research Infrastructure Programs (P40 OD010440). We thank Rocky Shi (BCCHR) for helping us develop the script to quantify gut granule number in the *C. elegans* intestine. Grant support was from The Canadian Institutes of Health Research (CIHR; PJT-153199 to ST), the Natural Sciences and Engineering Research Council of Canada (NSERC; RGPIN-2018-05133 to ST), the Cancer Research Society (CRS; to ST), and Diabetes Canada (OG-3-15-4946-FL to FL and ST). NS was supported by NSERC CGS-M and UBC Medical Genetics scholarships, AZK by a BCCHR Canucks for Kids Diabetes laboratory scholarship, JMG by a Vanier Canada Graduate Scholarship, MYYL by a BCCHR summer studentship, AM by an NSERC-USRA studentship, and ST by a Canada Research Chair. No author has any conflict of interest.

References

1. Hambidge KM, Miller LV, Westcott JE, Sheng X, Krebs NF. Zinc bioavailability and homeostasis. Am J Clin Nutr. 2010 May;91(5):1478S–1483S.

2. Vallee BL, Falchuk KH. The biochemical basis of zinc physiology. Physiol Rev. 1993 Jan;73(1):79–118.

3. Murakami M, Hirano T. Intracellular zinc homeostasis and zinc signaling. Cancer Sci. 2008 Aug;99(8):1515–22.

4. Andreini C, Banci L, Bertini I, Rosato A. Zinc through the three domains of life. J Proteome Res. 2006 Nov;5(11):3173–8.

5. Fukada T, Yamasaki S, Nishida K, Murakami M, Hirano T. Zinc homeostasis and signaling in health and diseases: Zinc signaling. J Biol Inorg Chem. 2011 Oct;16(7):1123–34.

6. Plum LM, Rink L, Haase H. The essential toxin: impact of zinc on human health. Int J Environ Res Public Health. 2010 Apr;7(4):1342–65.

7. Thévenod F, Lee W-K. Cadmium and cellular signaling cascades: interactions between cell death and survival pathways. Arch Toxicol. 2013 Oct;87(10):1743–86.

8. Joseph P. Mechanisms of cadmium carcinogenesis. Toxicol Appl Pharmacol. 2009 Aug 1;238(3):272–9.

9. Maret W. The Metals in the Biological Periodic System of the Elements: Concepts and Conjectures. Int J Mol Sci. 2016 Jan 5;17(1).

10. Dong J, Song MO, Freedman JH. Identification and characterization of a family of Caenorhabditis elegans genes that is homologous to the cadmium-responsive gene cdr-1. Biochim Biophys Acta. 2005 Jan 21;1727(1):16–26.

11. Brzóska MM, Moniuszko-Jakoniuk J. Interactions between cadmium and zinc in the organism. Food Chem Toxicol. 2001 Oct;39(10):967–80.

12. Park C, Jeong J. Synergistic cellular responses to heavy metal exposure: A minireview. Biochim Biophys Acta. 2018 Jul;1862(7):1584–91.

13. Dietrich N, Tan C-H, Cubillas C, Earley BJ, Kornfeld K. Insights into zinc and cadmium biology in the nematode Caenorhabditis elegans. Arch Biochem Biophys. 2016 Dec 1;611:120–33.

14. Chabosseau P, Rutter GA. Zinc and diabetes. Arch Biochem Biophys. 2016 Dec 1;611:79–85.

15. Ehrensberger KM, Bird AJ. Hammering out details: regulating metal levels in eukaryotes. Trends Biochem Sci. 2011 Oct;36(10):524–31.

16. Choi S, Bird AJ. Zinc'ing sensibly: controlling zinc homeostasis at the transcriptional level. Metallomics. 2014 Jul;6(7):1198–215.

17. Günther V, Lindert U, Schaffner W. The taste of heavy metals: gene regulation by MTF-1. Biochim Biophys Acta. 2012 Sep;1823(9):1416–25.

18. Coneyworth LJ, Jackson KA, Tyson J, Bosomworth HJ, van der Hagen E, Hann GM, et al. Identification of the human zinc transcriptional regulatory element (ZTRE): a palindromic protein-binding DNA sequence responsible for zinc-induced transcriptional repression. J Biol Chem. 2012 Oct 19;287(43):36567–81.

19. Roh HC, Dimitrov I, Deshmukh K, Zhao G, Warnhoff K, Cabrera D, et al. A modular system of DNA enhancer elements mediates tissue-specific activation of transcription by high dietary zinc in C. elegans. Nucleic Acids Res. 2015 Jan;43(2):803–16.

20. Warnhoff K, Roh HC, Kocsisova Z, Tan C-H, Morrison A, Croswell D, et al. The Nuclear Receptor HIZR-1 Uses Zinc as a Ligand to Mediate Homeostasis in Response to High Zinc. Sengupta P, Tissenbaum H, editors. PLoS Biol. Public Library of Science; 2017 Jan;15(1):e2000094.

21. Taubert S, Ward JD, Yamamoto KR. Nuclear hormone receptors in nematodes: evolution and function. Mol Cell Endocrinol. 2011 Mar 1;334(1-2):49–55.

22. O'Malley BW, Qin J, Lanz RB. Cracking the coregulator codes. Current Opinion in Cell Biology. 2008 Jun;20(3):310–5.

23. Spiegelman BM, Heinrich R. Biological control through regulated transcriptional coactivators. Cell. 2004 Oct 15;119(2):157–67.

24. Vihervaara A, Duarte FM, Lis JT. Molecular mechanisms driving transcriptional stress responses. Nat Rev Genet. 2018 Jun;19(6):385–97.

25. Allen BL, Taatjes DJ. The Mediator complex: a central integrator of transcription. Nat Rev Mol Cell Biol. 2015 Mar;16(3):155–66.

26. Grants JM, Goh GYS, Taubert S. The Mediator complex of Caenorhabditis elegans: insights into the developmental and physiological roles of a conserved transcriptional coregulator. Nucleic Acids Res. 2015 Feb 27;43(4):2442–53.

27. Naar AM, Thakur JK. Nuclear receptor-like transcription factors in fungi. Genes Dev. 2009 Feb 15;23(4):419–32.

28. Nishikawa JL, Boeszoermenyi A, Vale-Silva LA, Torelli R, Posteraro B, Sohn Y-J, et al. Inhibiting fungal multidrug resistance by disrupting an activator-Mediator interaction. Nature. 2016 Feb 25;530(7591):485–9.

29. Fant CB, Taatjes DJ. Regulatory functions of the Mediator kinases CDK8 and CDK19. transcription. 2018 Dec 26;153(6):1–15.

30. Galbraith MD, Allen MA, Bensard CL, Wang X, Schwinn MK, Qin B, et al. HIF1A employs CDK8-mediator to stimulate RNAPII elongation in response to hypoxia. Cell. 2013 Jun 6;153(6):1327–39.

31. Bose S, Dutko JA, Zitomer RS. Genetic factors that regulate the attenuation of the general stress response of yeast. Genetics. 2005 Mar;169(3):1215–26.

32. Marr MT, Isogai Y, Wright KJ, Tjian R. Coactivator cross-talk specifies transcriptional output. Genes Dev. 2006 Jun 1;20(11):1458–69.

33. Taubert S, Hansen M, Van Gilst MR, Cooper SB, Yamamoto KR. The Mediator subunit MDT-15 confers metabolic adaptation to ingested material. PLoS Genet. 2008 Feb;4(2):e1000021.

34. Taubert S, Van Gilst MR, Hansen M, Yamamoto KR. A Mediator subunit, MDT-15, integrates regulation of fatty acid metabolism by NHR-49-dependent and -independent pathways in C. elegans. Genes Dev. 2006 May 1;20(9):1137–49.

35. Arda HE, Taubert S, Macneil LT, Conine CC, Tsuda B, Van Gilst M, et al. Functional modularity of nuclear hormone receptors in a Caenorhabditis elegans metabolic gene regulatory network. Molecular Systems Biology. 2010 May 11;6:367.

36. Goh GYS, Winter JJ, Bhanshali F, Doering KRS, Lai R, Lee K, et al. NHR-49/HNF4 integrates regulation of fatty acid metabolism with a protective transcriptional response to oxidative stress and fasting. Aging Cell. 2018 Jun;17(3):e12743.

37. Hu Q, D'Amora DR, Macneil LT, Walhout AJM, Hu Q. The Caenorhabditis elegans Oxidative Stress Response Requires the NHR-49 Transcription Factor. G3 (Bethesda). 2018 Dec 10;8(12):3857–63.

38. Liao VH-C, Dong J, Freedman JH. Molecular characterization of a novel, cadmium-inducible gene from the nematode Caenorhabditis elegans. A new gene that contributes to the resistance to cadmium toxicity. J Biol Chem. 2002 Nov 1;277(44):42049–59.

39. Kormish JD, Gaudet J, Mcghee JD. Development of the C. elegans digestive tract. Current Opinion in Genetics & Development. 2010 Aug;20(4):346–54.

40. Svensk E, Ståhlman M, Andersson C-H, Johansson M, Borén J, Pilon M. PAQR-2 Regulates Fatty Acid Desaturation during Cold Adaptation in C. elegans. PLoS Genet. 2013 Sep;9(9):e1003801.

41. Lee D, An S, Jung Y, Yamaoka Y, Ryu Y, Goh G, et al. C. elegans Mediator 15 permits low temperature-induced longevity via regulation of lipid and protein homeostasis. biorxivorg.

42. Goh GYS, Martelli KL, Parhar KS, Kwong AWL, Wong MA, Mah A, et al. The conserved Mediator subunit MDT-15 is required for oxidative stress responses in Caenorhabditis elegans. Aging Cell. 2014 Feb;13(1):70–9.

43. Yang F, Vought BW, Satterlee JS, Walker AK, Jim Sun Z-Y, Watts JL, et al. An ARC/Mediator subunit required for SREBP control of cholesterol and lipid homeostasis. Nature. 2006 Aug 10;442(7103):700–4.

44. Roh HC, Collier S, Guthrie J, Robertson JD, Kornfeld K. Lysosome-related organelles in intestinal cells are a zinc storage site in C. elegans. Cell Metabolism. 2012 Jan 4;15(1):88–99.

45. Lee D, Jeong D-E, Son HG, Yamaoka Y, Kim H, Seo K, et al. SREBP and MDT-15 protect C. elegans from glucose-induced accelerated aging by preventing accumulation of saturated fat. Genes Dev. 2015 Dec 1;29(23):2490–503.

46. Hou NS, Gutschmidt A, Choi DY, Pather K, Shi X, Watts JL, et al. Activation of the endoplasmic reticulum unfolded protein response by lipid disequilibrium without disturbed proteostasis in vivo. Proc Natl Acad Sci USA. 2014 Jun 3;111(22):E2271–80.

47. Brock TJ, Browse J, Watts JL. Genetic regulation of unsaturated fatty acid composition in C. elegans. PLoS Genet. 2006 Jul;2(7):e108.

48. Bourbon H-M, Aguilera A, Ansari AZ, Asturias FJ, Berk AJ, Björklund S, et al. A unified nomenclature for protein subunits of mediator complexes linking transcriptional regulators to RNA polymerase II. Molecular Cell. 2004 Jun 4;14(5):553–7.

49. IARC Working Group on the Evaluation of Carcinogenic Risks to Humans. Arsenic, metals, fibres, and dusts. IARC Monogr Eval Carcinog Risks Hum. 2012;100(Pt C):11–465.

50. Beveridge R, Pintos J, Parent M-É, Asselin J, Siemiatycki J. Lung cancer risk associated with occupational exposure to nickel, chromium VI, and cadmium in two population-based case-control studies in Montreal. Am J Ind Med. 2010 May;53(5):476–85.

51. Zhao W-J, Zhang Z-J, Zhu Z-Y, Song Q, Zheng W-J, Hu X, et al. Time-dependent response of A549 cells upon exposure to cadmium. J Appl Toxicol. 2018 Jul 26;:1–10.

52. Rutter GA, Chabosseau P, Bellomo EA, Maret W, Mitchell RK, Hodson DJ, et al. Intracellular zinc in insulin secretion and action: a determinant of diabetes risk? Proc Nutr Soc. 2016 Feb;75(1):61–72.

53. Li YV. Zinc and insulin in pancreatic beta-cells. Endocrine. 2014 Mar;45(2):178–89.

54. Chen W, Roeder RG. Mediator-dependent nuclear receptor function. Seminars in Cell and Developmental Biology. 2011 Sep;22(7):749–58.

55. Mao X, Kim B-E, Wang F, Eide DJ, Petris MJ. A histidine-rich cluster mediates the ubiquitination and degradation of the human zinc transporter, hZIP4, and protects against zinc cytotoxicity. J Biol Chem. American Society for Biochemistry and Molecular Biology; 2007 Mar 9;282(10):6992–7000.

56. Bafaro E, Liu Y, Xu Y, Dempski RE. The emerging role of zinc transporters in cellular homeostasis and cancer. Signal Transduct Target Ther. 2017;2:17029.

57. Thakur JK, Arthanari H, Yang F, Chau KH, Wagner G, Näär AM. Mediator subunit Gal11p/MED15 is required for fatty acid-dependent gene activation by yeast transcription factor Oaf1p. J Biol Chem. 2009 Feb 13;284(7):4422–8.

58. Thakur JK, Arthanari H, Yang F, Pan S-J, Fan X, Breger J, et al. A nuclear receptor-like pathway regulating multidrug resistance in fungi. Nature. 2008 Apr 3;452(7187):604–9.

59. Lee K, Goh GYS, Wong MA, Klassen TL, Taubert S. Gain-of-Function Alleles in Caenorhabditis elegans Nuclear Hormone Receptor nhr-49 Are Functionally Distinct. PLoS ONE. 2016;11(9):e0162708.

60. Yamazaki K, Kuromitsu J, Tanaka I. Microarray analysis of gene expression changes in mouse liver induced by peroxisome proliferator- activated receptor alpha agonists. Biochem Biophys Res Commun. 2002 Jan 25;290(3):1114–22.

61. Grants JM, Ying LTL, Yoda A, You CC, Okano H, Sawa H, et al. The Mediator Kinase Module Restrains Epidermal Growth Factor Receptor Signaling and Represses Vulval Cell Fate Specification in Caenorhabditis elegans. Genetics. Genetics; 2016 Feb;202(2):583–99.

62. Cui Y, McBride SJ, Boyd WA, Alper S, Freedman JH. Toxicogenomic analysis of Caenorhabditis elegans reveals novel genes and pathways involved in the resistance to cadmium toxicity. Genome Biol. BioMed Central Ltd; 2007;8(6):R122.

63. Brenner S. The genetics of Caenorhabditis elegans. Genetics. 1974 May;77(1):71–94.

64. Untergasser A, Cutcutache I, Koressaar T, Ye J, Faircloth BC, Remm M, et al. Primer3--new capabilities and interfaces. Nucleic Acids Res. 2012 Aug;40(15):e115–5.

65. Stuart GW, Searle PF, Chen HY, Brinster RL, Palmiter RD. A 12-base-pair DNA motif that is repeated several times in metallothionein gene promoters confers metal regulation to a heterologous gene. Proceedings of the National Academy of Sciences. 1984 Dec;81(23):7318–22.

66. Sorger PK. Heat shock factor and the heat shock response. Cell. 1991 May 3;65(3):363–6.

67. Blackwell TK, Bowerman B, Priess JR, Weintraub H. Formation of a monomeric DNA binding domain by Skn-1 bZIP and homeodomain elements. Science. 1994 Oct 28;266(5185):621–8.

68. Chen X, Chu M, Giedroc DP. MRE-Binding transcription factor-1: weak zinc-binding finger domains 5 and 6 modulate the structure, affinity, and specificity of the metal-response element complex. Biochemistry. 1999 Sep 28;38(39):12915–25.

69. Furuyama T, Nakazawa T, Nakano I, Mori N. Identification of the differential distribution patterns of mRNAs and consensus binding sequences for mouse DAF-16 homologues. Biochem J. Portland Press Ltd; 2000 Jul 15;349(Pt 2):629–34.

70. Smale ST, Kadonaga JT. The RNA polymerase II core promoter. Annu Rev Biochem. 2003;72:449–79.

71. An JH, Blackwell TK. SKN-1 links C. elegans mesendodermal specification to a conserved oxidative stress response. Genes Dev. 2003 Aug 1;17(15):1882–93.

72. Shen C, Nettleton D, Jiang M, Kim SK, Powell-Coffman JA. Roles of the HIF-1 hypoxia-inducible factor during hypoxia response in Caenorhabditis elegans. J Biol Chem. 2005 May 27;280(21):20580–8.

73. Mcghee JD, Sleumer MC, Bilenky M, Wong K, McKay SJ, Goszczynski B, et al. The ELT-2 GATA-factor and the global regulation of transcription in the C. elegans intestine. Dev Biol. 2007 Feb 15;302(2):627–45.

74. Chiang W-C, Ching T-T, Lee HC, Mousigian C, Hsu A-L. HSF-1 regulators DDL-1/2 link insulin-like signaling to heat-shock responses and modulation of longevity. Cell. 2012 Jan 20;148(1-2):322–34.

75. Rueden CT, Schindelin J, Hiner MC, DeZonia BE, Walter AE, Arena ET, et al. ImageJ2: ImageJ for the next generation of scientific image data. BMC Bioinformatics. 2017 Nov 29;18(1):529.

76. Sabatini PV, Speckmann T, Nian C, Glavas MM, Wong CK, Yoon JS, et al. Neuronal PAS Domain Protein 4 Suppression of Oxygen Sensing Optimizes Metabolism during Excitation of Neuroendocrine Cells. Cell Rep. 2018 Jan 2;22(1):163–74.

77. Johnson DS, Mortazavi A, Myers RM, Wold B. Genome-wide mapping of in vivo protein-DNA interactions. Science. 2007 Jun 8;316(5830):1497–502.

747 **Supporting Information**

748 Table S1: List of worm strains.

749 Table S2: List of HT115 RNAi bacteria clones from the Ahringer library.

750 Table S3: List of primers used in qPCR experiments.

751 Figure S1: The *cdr-1p::gfp* transcriptional reporter is induced by 100µM cadmium and 200µM

752 zinc, and induction in adult worms by cadmium requires *elt-2*.

753 Figure S2: MDT-15 and HIZR-1 interact physically.

754 Figure S3: *mdt-15(tm2182)* and *hizr-1(am286)* mutants have a zinc storage defect.

755 Figure S4: Expression analysis of fusion proteins for Y2H assays.

756

Figure legends

Figure 1: Mediator subunits *mdt-15* and *cdk-8* are required for heavy metal stress responses. [A] The Venn diagram depicts the overlap between genes downregulated in the *mdt-15(tm2182)* mutant and genes induced by cadmium (from (62)). Statistical significance was assessed by Fisher's exact test. **[B]** The Venn diagram depicts the overlap between genes downregulated in the *cdk-8(tm1238)* mutant and genes induced by cadmium. Statistical significance was assessed by Fisher's exact test. **[C-D]** qPCR analysis of zinc and cadmium-responsive genes in wild-type (WT) and *cdk-8(tm1238)* mutant worms grown on 100µM cadmium for 4 hours [C] or on 200µM zinc for 16 hours [D]. Graphs show fold induction, normalized to the average of unsupplemented WT mRNA levels. Error bars: SEM (n=3). Statistical analysis: * $p < 0.05$, unpaired t-test comparing WT supplemented worms to mutant supplemented worms.

Figure 2: The TFs *hizr-1* and *elt-2* and their cognate promoter elements are required for heavy metal stress responses. [A] Illustration of the *cdr-1p::gfp* reporter and putative regulatory DNA elements in the *cdr-1* promoter; note, the diagram is not to scale. For details, see text. **[B]** Graphs show average fluorescence intensity (arbitrary units, A.U.) of worms bearing the *cdr-1p::gfp* transcriptional reporter in WT and *cdk-8(tm1238)* backgrounds or fed either control or *mdt-15* RNAi and exposed for four hours to 0µM or 100µM cadmium or 0µM or 200µM zinc, as indicated. Error bars: SEM ($n > 19$ worms per group). Statistical analysis: **** $p < 0.0001$, n.s.= not significant, Two-way ANOVA, multiple comparisons, Tukey correction; comparisons are to WT or *control(RNAi)* unless indicated. **[C]** Graph shows average fluorescence intensity (arbitrary units, A.U.) of worms bearing the *cdr-1p::gfp* transcriptional reporter before and after a 0µM or 100µM cadmium exposure (four hours), and fed either control or transcription factor RNAi, as indicated. Error bars: SEM ($n > 19$ worms per group). Statistical analysis: **** $p < 0.0001$, n.s.= not significant, Two-way ANOVA, multiple comparisons, Tukey correction; comparisons are to *control(RNAi)* unless indicated. **[D]** Graph shows average

fluorescence intensity (arbitrary units, A.U.) of worms bearing the following *cdr-1p::gfp* reporter variants: wild-type, WT; mutated HZA element, *cdr-1PΔHZA*; mutated GATA elements, *cdr-1PΔGATA1* or *cdr-1PΔGATA2*. All mutants were assessed with 0µM or 100µM cadmium (four hours). Error bars: SEM ($n > 19$ worms per group). Statistical analysis: **** $p < 0.0001$, n.s.= not significant, Two-way ANOVA, multiple comparisons, Tukey correction; comparisons are to WT unless indicated.

Figure 3: MDT-15 and HIZR-1 are co-dependent for metal responsive gene induction and physically bind in zinc-enhanced fashion. [A-B] qPCR analysis of zinc and cadmium-responsive genes. The graphs show fold-inductions of mRNAs normalized to the average of wild-type *control(RNAi)* worms. Error bars: SEM. Statistical analysis: * $p < 0.05$, ** $p < 0.01$, unpaired Student's t-test for indicated comparisons. [A] Comparison of wild-type and *hizr-1(am285)* worms grown on control RNAi or *mdt-15* RNAi (n=5). [B] Comparison of wild-type and *mdt-15(yh8)* worms grown on control RNAi, *hizr-1* RNAi, or *nhr-49* RNAi (n= 3). **[C-E]** Protein-protein interaction analysis using the Y2H system. Graphs show average interaction strength (arbitrary units, A.U.). Error bars: SEM. [C] Interaction between MDT-15 and HIZR-1, with Empty Vector (EV)-HIZR-1 and MDT-15-EV as negative controls, and MDT-15–SKN-1c as a positive control (n=3). Statistical analysis: *** p < 0.001, **** p < 0.0001, One-way ANOVA, multiple comparisons, Dunnett correction. All comparisons for "MDT-15 + EV" unless indicated. [D] Interaction strength between MDT-15 and HIZR-1; MDT-15 and NHR-64; and MDT-15 and NHR-49, all with no treatment, or treated with 200µM zinc, 5µM cadmium, or 200µM manganese (n=3). Statistical analysis: **** p < 0.0001, Two-way ANOVA, multiple comparisons, Dunnett correction. All comparisons to the pertinent "no supplement" control. [E] Interaction between HIZR-1 and MDT-15 or HIZR-1-D270N and MDT-15 with and without zinc treatment (n=4). Statistical analysis: ** p < 0.01, *** p < 0.001, One-way ANOVA, multiple comparisons, Dunnett correction. All comparisons to "HIZR-1" unless indicated.

Figure 4: *mdt-15(tm2182)* mutants have a zinc storage defect and are sensitive to excess heavy metals. [A] Representative fluorescence images of worms stained with FluoZin-3, showing zinc accumulation in gut granules in wild-type, *mdt-15(tm2182)*, *cdk-8(tm1238)*, and *hizr-1(am286)* worms grown with 200µM zinc supplementation. **[B]** Quantification of the number of gut granules in wild-type (WT), *mdt-15(tm2182)*, and *cdk-8(tm1238)* worms; every dot represents an individual worm. Error bars: SEM. $n > 10$ worms per genotype. Statistical analysis: **** $p < 0.0001$, One-way ANOVA, multiple comparisons, Dunnett correction, compared to "WT". **[C]** Quantification of the number of gut granules in WT and *hizr-1(am286)* worms; every dot represents an individual worm. Error bars: SEM. $n > 13$ worms per genotype. Statistical analysis: *** $p < 0.001$, One-way ANOVA, multiple comparisons, Dunnett correction, compared to "WT". **[D]** Graphs show the average number of eggs laid over a 24-hour period by WT worms and *mdt-15(tm2182)* mutants grown on 0µM and 100µM zinc ($n > 51$ worms per condition). Error bars: SEM; statistical analysis: **** $p < 0.0001$ Two-way ANOVA, multiple comparisons; Tukey correction. **[E]** Graphs show the average number of eggs laid over a 24-hour period by WT worms and *mdt-15(tm2182)* mutants grown on 0µM and 2.5µM cadmium ($n > 23$ worms per condition). Error bars: SEM; statistical analysis: **** $p < 0.0001$ Two-way ANOVA, multiple comparisons; Tukey correction.

Figure 5. MED15 binds and regulates metal responsive genes in mammalian cells. [A] qPCR analysis of cadmium inducible genes in control (scr = scrambled siRNA) and MED15 siRNA (siMED15) treated A549 cells exposed to 5µM cadmium for four hours. MT1X was not affected in statistically significant fashion. For MT2A, all comparisons are *vs.* the untreated scr samples except where indicated. Error bars: SEM; statistical analysis: * $p < 0.05$, ** $p < 0.01$ Two-way ANOVA, multiple comparisons, Tukey correction (n=3). **[B]** The graph shows relative MED15 occupancy at the MT1X and MT2A promoters and nearby control regions in A549 cells, as determined by ChIP-qPCR before and after the addition of 5µM cadmium. Error bars: SEM; statistical analysis: ** $p < 0.01$

Student's T-test, multiple comparisons, Holm-Sidak correction (n=3). **[C]** The graph shows qPCR analysis of MIN6 cells treated without and with 50μM zinc. Error bars: SEM; statistical analysis: ** $p < 0.01$, *** $p < 0.001$ Student's T-test, multiple comparisons, Holm-Sidak correction (n=4). **[D]** The graph shows relative Med15 occupancy at the *Mt1* promoter and Slc30a8 enhancer and nearby control regions in MIN6 cells as determined by ChIP-qPCR, before and after the addition of 100μM Zn. Error bars: SEM; statistical analysis: * $p < 0.05$, *** $p < 0.01$ Student's T-test, multiple comparisons, Holm-Sidak correction (n=3).

Figure 6. Model of MDT-15 and MED15 driven gene regulation in response to high metal levels. [A] In the *C. elegans* intestinal cells, MDT-15 cooperates with HIZR-1 bound to the HZA element to induce the metal sequestering metallothioneins (*mtl-1* and *-2*) and the transporter *cdf-2*, which shuttles zinc into storage granules; excess cadmium is likely detoxified through similar mechanisms. ELT-2 may also contact Mediator to regulate metal responsive transcription. **[B]** In the mouse pancreatic β-cells, Med15 regulates the expression of genes such as Slc30a8/ZnT1 in response to elevated zinc levels, possibly via HNF4, or other, Mediator contacting proteins.

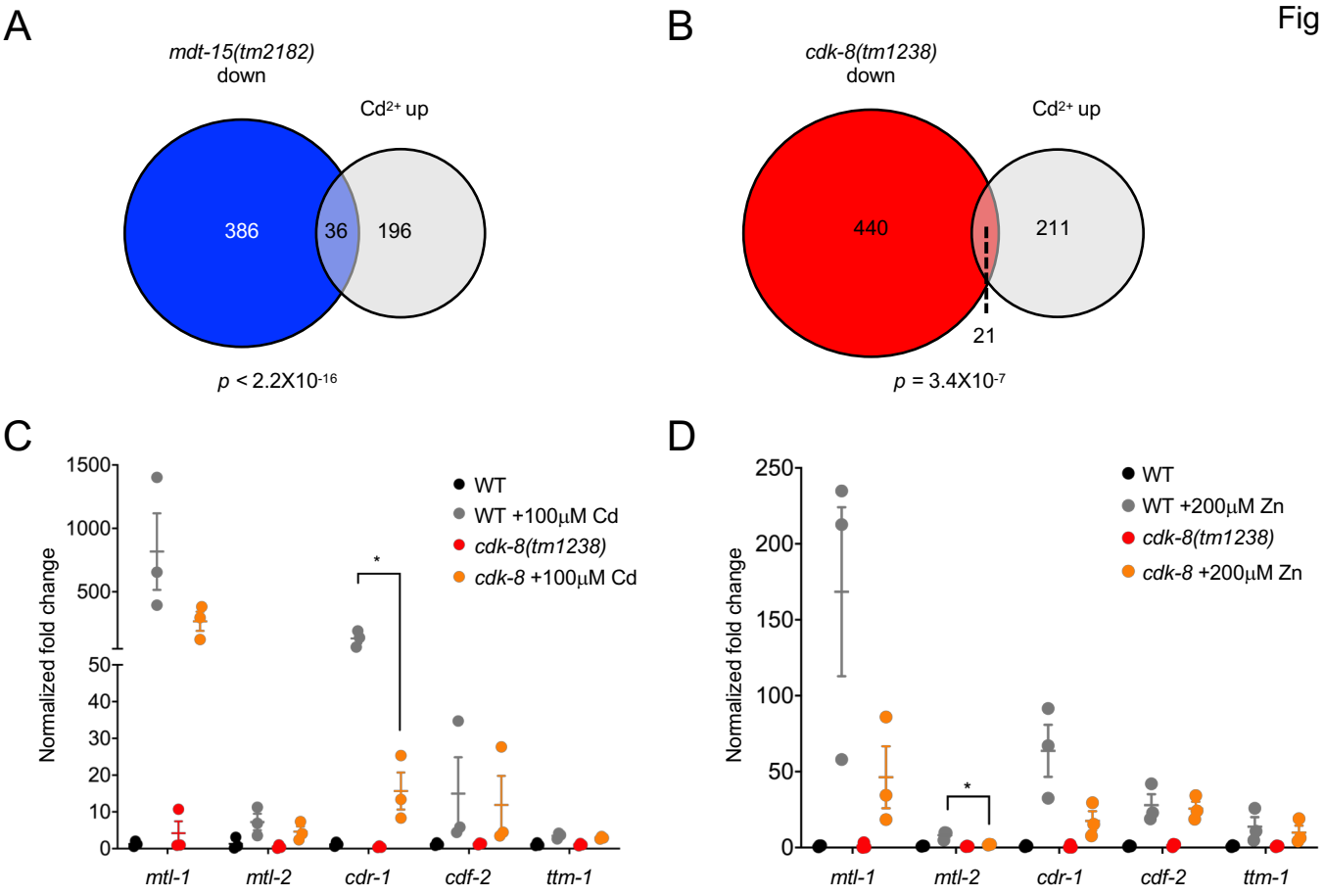
A
mdt-15(tm2182)
down
Cd2+ up
386
36
196
p < 2.2X10-16
B
cdk-8(tm1238)
down
Cd2+ up
440
211
21
p = 3.4X10-7
C
Normalized fold change
1500
1000
500
50
40
30
20
10
0
WT
WT +100μM Cd
cdk-8(tm1238)
cdk-8 +100μM Cd
*
mtl-1
mtl-2
cdr-1
cdf-2
ttm-1
D
Normalized fold change
250
200
150
100
50
0
WT
WT +200μM Zn
cdk-8(tm1238)
cdk-8 +200μM Zn
*
mtl-1
mtl-2
cdr-1
cdf-2
ttm-1

A

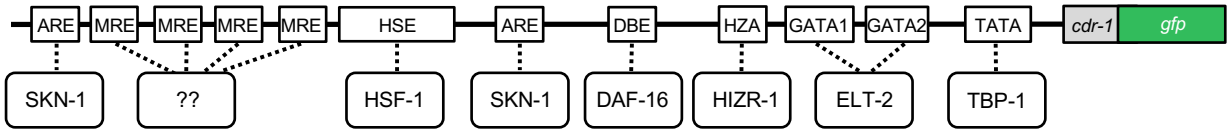
ARE
MRE
MRE
MRE
MRE
HSE
ARE
DBE
HZA
GATA1
GATA2
TATA
cdr-1
gfp
SKN-1
??
HSF-1
SKN-1
DAF-16
HIZR-1
ELT-2
TBP-1

B

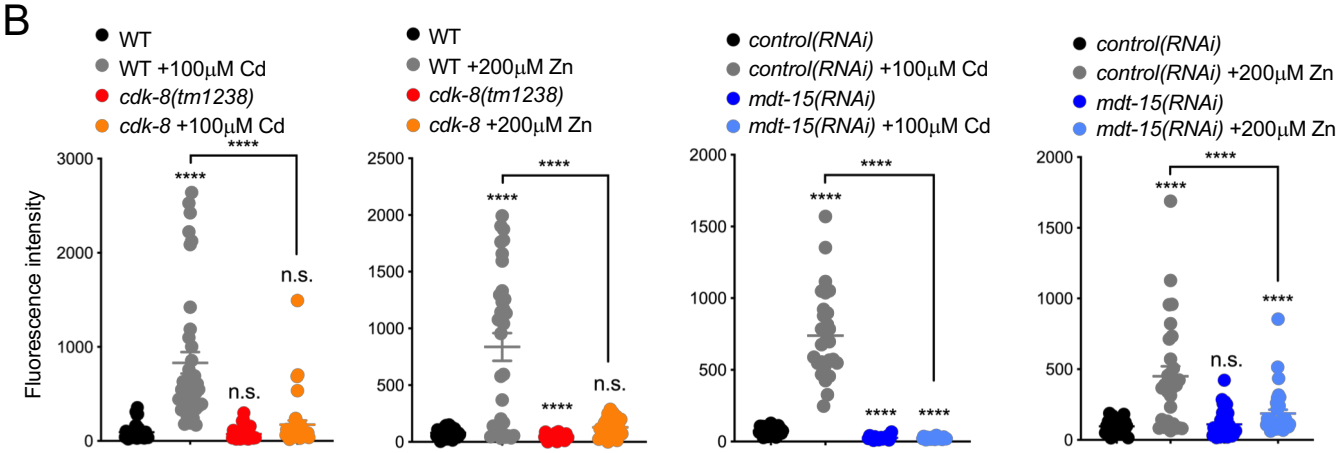
WT
WT +100μM Cd
cdk-8(tm1238)
cdk-8 +100μM Cd
WT
WT +200μM Zn
cdk-8(tm1238)
cdk-8 +200μM Zn
control(RNAi)
control(RNAi) +100μM Cd
mdt-15(RNAi)
mdt-15(RNAi) +100μM Cd
control(RNAi)
control(RNAi) +200μM Zn
mdt-15(RNAi)
mdt-15(RNAi) +200μM Zn
Fluorescence intensity
****
n.s.

C

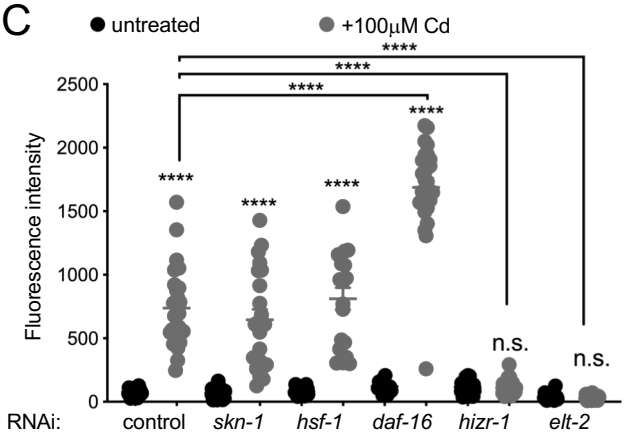
untreated
+100μM Cd
Fluorescence intensity
****
n.s.
RNAi:
control
skn-1
hsf-1
daf-16
hizr-1
elt-2

D

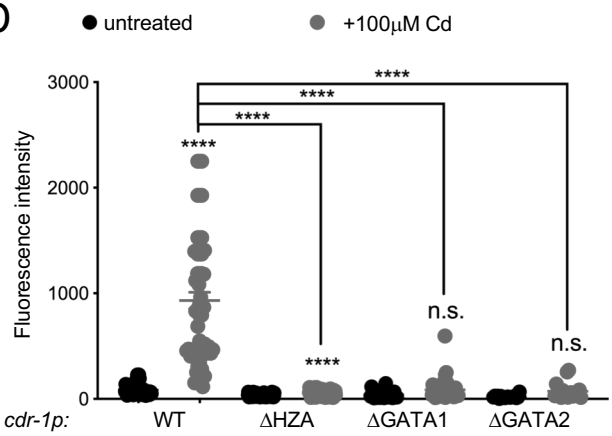
untreated
+100μM Cd
Fluorescence intensity
****
n.s.
cdr-1p:
WT
ΔHZA
ΔGATA1
ΔGATA2

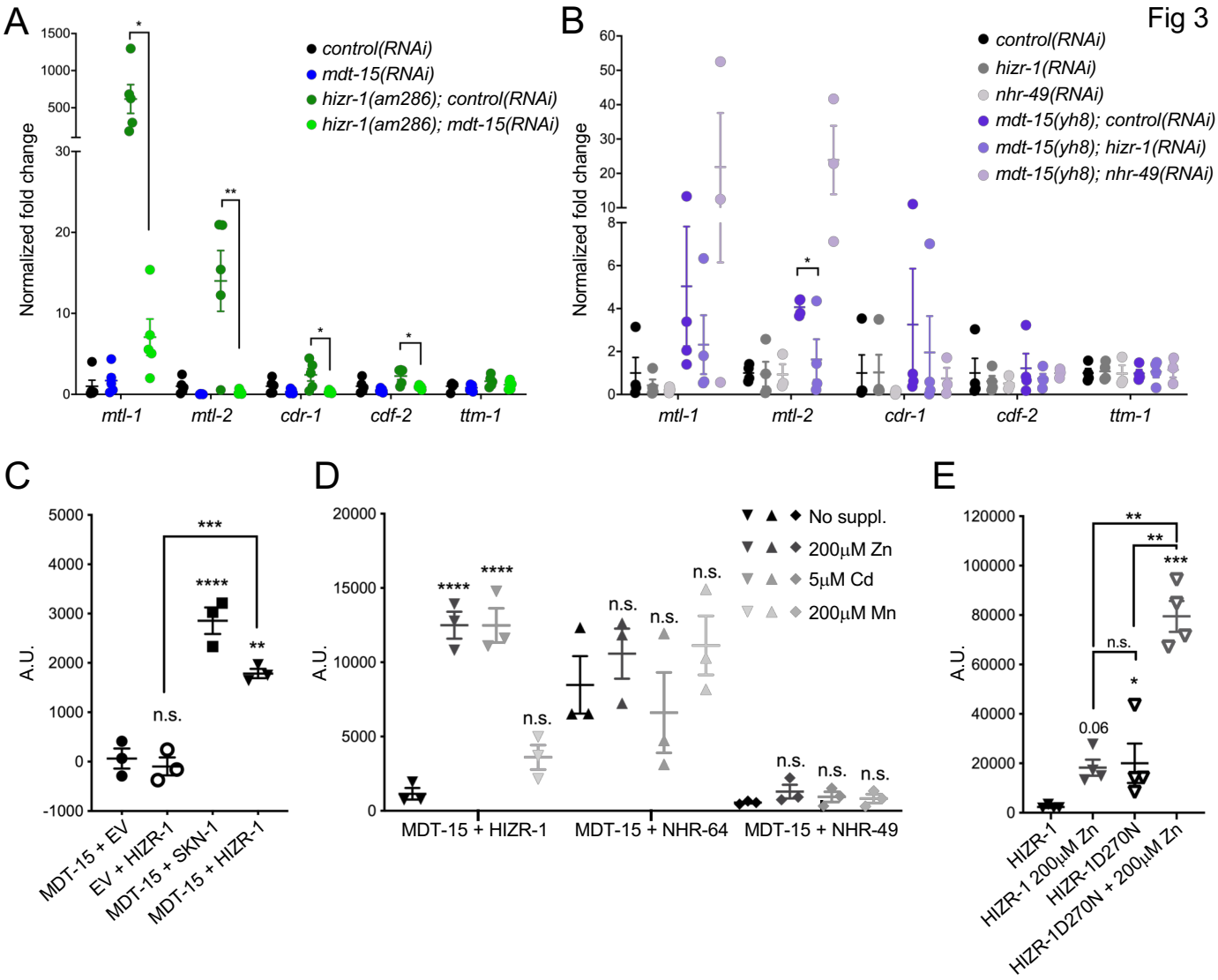
A
Normalized fold change
control(RNAi)
mdt-15(RNAi)
hizr-1(am286); control(RNAi)
hizr-1(am286); mdt-15(RNAi)
mtl-1
mtl-2
cdr-1
cdf-2
ttm-1
B
Normalized fold change
control(RNAi)
hizr-1(RNAi)
nhr-49(RNAi)
mdt-15(yh8); control(RNAi)
mdt-15(yh8); hizr-1(RNAi)
mdt-15(yh8); nhr-49(RNAi)
mtl-1
mtl-2
cdr-1
cdf-2
ttm-1
C
A.U.
MDT-15 + EV
EV + HIZR-1
MDT-15 + SKN-1
MDT-15 + HIZR-1
D
A.U.
No suppl.
200μM Zn
5μM Cd
200μM Mn
MDT-15 + HIZR-1
MDT-15 + NHR-64
MDT-15 + NHR-49
E
A.U.
HIZR-1
HIZR-1 200μM Zn
HIZR-1D270N
HIZR-1D270N + 200μM Zn

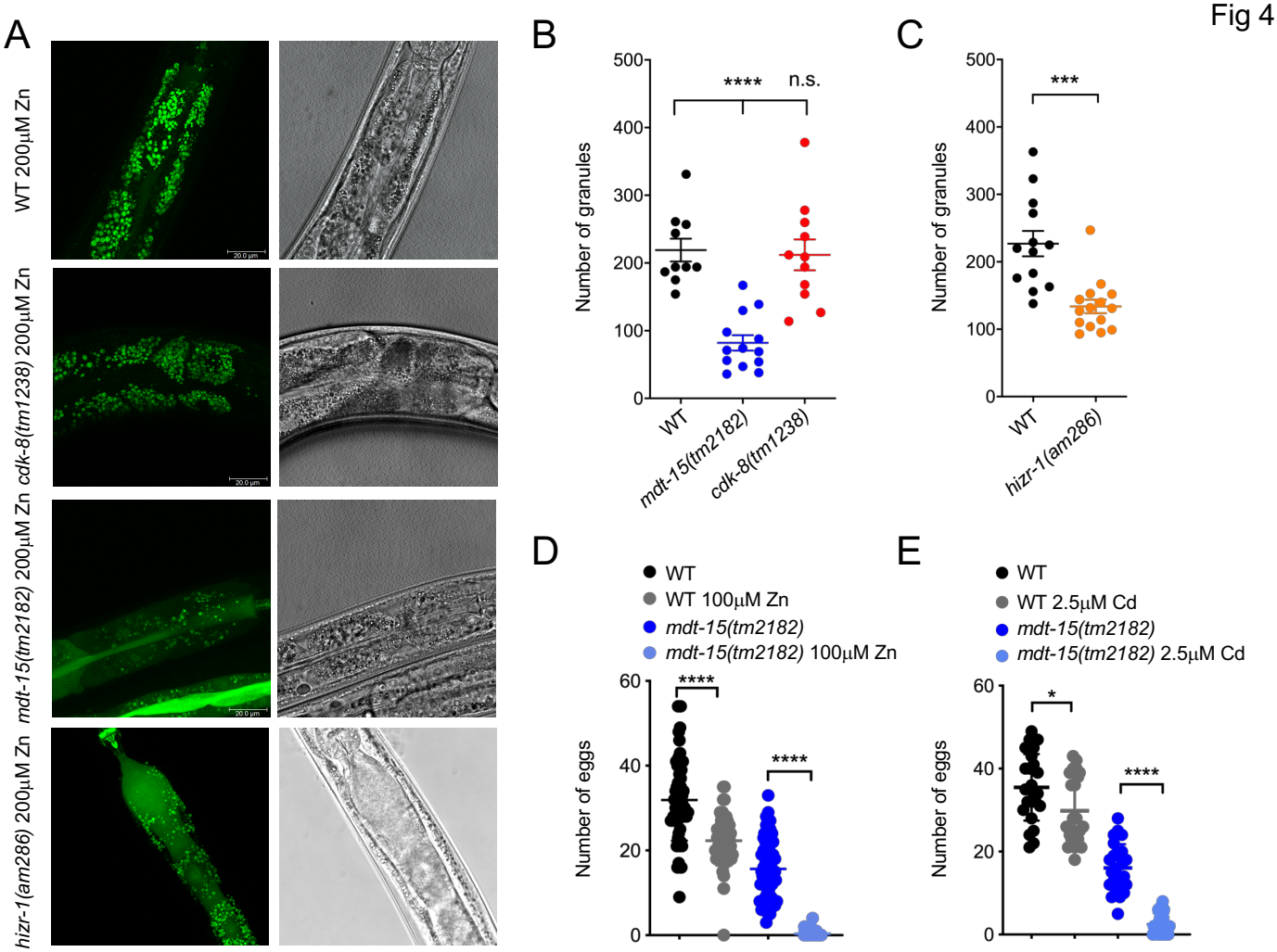
A
WT 200µM Zn
cdk-8(tm1238) 200µM Zn
mdt-15(tm2182) 200µM Zn
hizr-1(am286) 200µM Zn
B
Number of granules
****
n.s.
WT
mdt-15(tm2182)
cdk-8(tm1238)
C
Number of granules
***
WT
hizr-1(am286)
D
WT
WT 100µM Zn
mdt-15(tm2182)
mdt-15(tm2182) 100µM Zn
Number of eggs
****
****
E
WT
WT 2.5µM Cd
mdt-15(tm2182)
mdt-15(tm2182) 2.5µM Cd
Number of eggs
*
****

A

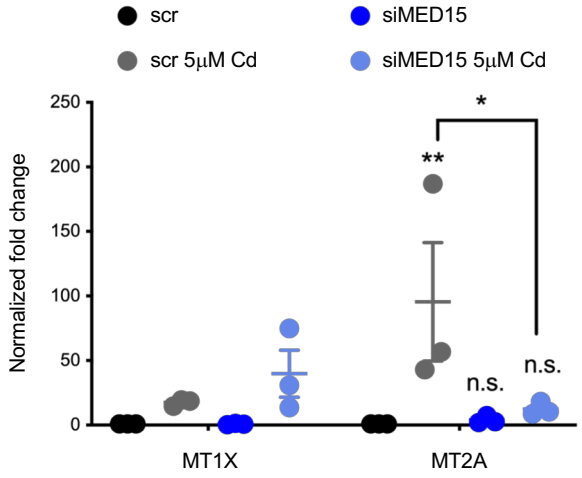
scr
siMED15
scr 5μM Cd
siMED15 5μM Cd
Normalized fold change
250
200
150
100
50
0
**
*
n.s.
n.s.
MT1X
MT2A

B

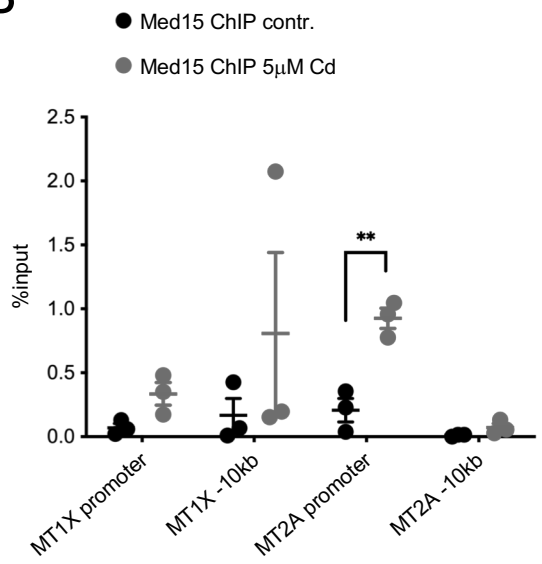
Med15 ChIP contr.
Med15 ChIP 5μM Cd
%input
2.5
2.0
1.5
1.0
0.5
0.0
**
MT1X promoter
MT1X -10kb
MT2A promoter
MT2A -10kb

C

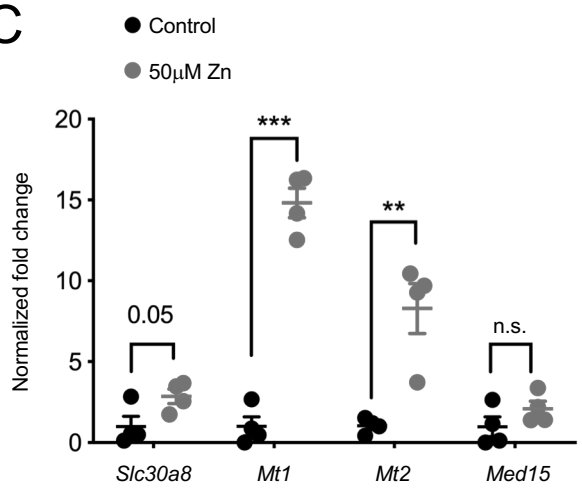
Control
50μM Zn
Normalized fold change
20
15
10
5
0
0.05
***
**
n.s.
Slc30a8
Mt1
Mt2
Med15

D

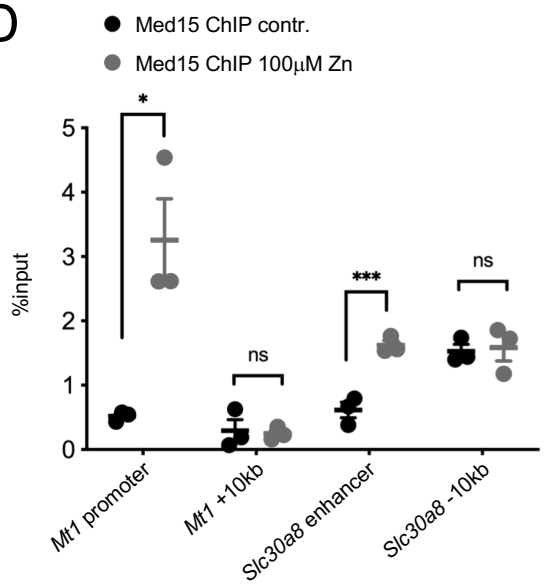
Med15 ChIP contr.
Med15 ChIP 100μM Zn
%input
5
4
3
2
1
0
*
ns
***
ns
Mt1 promoter
Mt1 +10kb
Slc30a8 enhancer
Slc30a8 -10kb

A

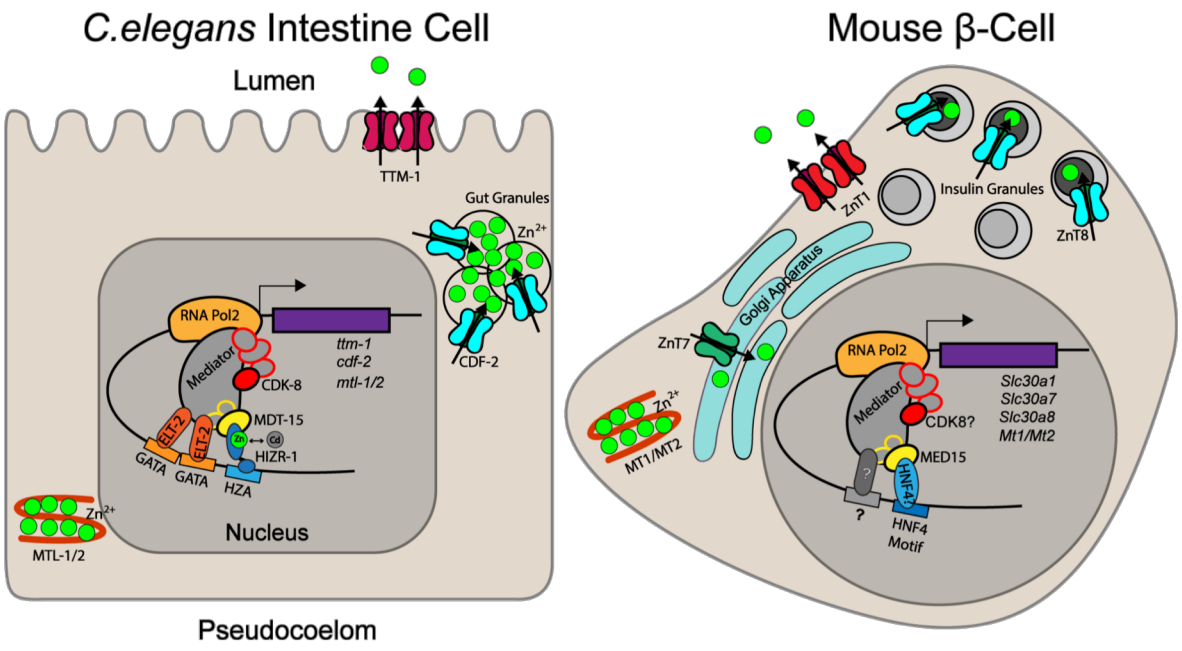
C.elegans Intestine Cell
Lumen
TTM-1
Gut Granules
Zn2+
CDF-2
RNA Pol2
Mediator
CDK-8
ttm-1
cdf-2
mtl-1/2
MDT-15
ELT-2
ELT-2
GATA
GATA
HIZR-1
HZA
Nucleus
Zn2+
MTL-1/2
Pseudocoelom
Mouse β-Cell
ZnT1
Insulin Granules
ZnT8
Golgi Apparatus
ZnT7
Zn2+
MT1/MT2
RNA Pol2
Mediator
CDK8?
Slc30a1
Slc30a7
Slc30a8
Mt1/Mt2
MED15
HNF4
?
HNF4
Motif